



Article

Biosynthesis and Characterization of Copper Nanoparticles Using a Biofloculant Produced by a Yeast *Pichia kudriavzevii* Isolated from Kombucha Tea SCOBY

Phakamani H. Tsilo ¹, Albertus K. Basson ¹, Zuzingcebo G. Ntombela ¹, Nkosinathi G. Dlamini ¹ and Rajasekhar V. S. R. Pullabhotla ^{2,*}

¹ Department of Biochemistry and Microbiology, Faculty of Science, Agriculture and Engineering, University of Zululand, P/Bag X1001, Kwadlangezwa 3886, South Africa

² Department of Chemistry, Faculty of Science, Agriculture and Engineering, University of Zululand, P/Bag X1001, Kwadlangezwa 3886, South Africa

* Correspondence: pullabhotlav@unizulu.ac.za; Tel.: +27-35-902-6155; Fax: +27-35-902-6568

Abstract: Over recent years, the ‘green’ chemistry approach to synthesizing nanoparticles has made significant developments. Because of their unique features, nanoparticles have received a lot of attention. The use of a biofloculant to promote the environmentally friendly synthesis of copper nanoparticles is described in this paper. Copper nanoparticles were biosynthesized using biofloculant which was produced from a yeast, *Pichia kudriavzevii*. The chemical reduction approach was used to synthesize copper nanoparticles (CuNPs) using a biofloculant as a capping agent. Characterization of the as-synthesized copper nanoparticles was conducted using Fourier transform infrared (FT-IR) spectroscopy, UV-visible spectroscopy, X-ray diffraction (XRD), transmission electron microscopy (TEM), scanning electron microscopy (SEM), and energy dispersive X-ray (EDX). The FT-IR spectra revealed characteristic peaks at 3267, 2956, 1656, 1059, and 511 cm⁻¹ for the biofloculant, while for the biofloculant passivated CuNPs, the characteristic peaks were at 3482 (-OH), 3261, 1640, 1059, 580, and 519 cm⁻¹ (Cu-O). These peaks revealed that functional groups such as hydroxyls, amines, and copper oxide bonds were present. The UV-Vis analysis showed surface plasmon resonance (SPR) at an absorbance range of 500–600 nm, with peak maxima at 555 and 575 nm for the as-synthesized CuNPs. The XRD pattern revealed planes such as (200) and (220) at $2\theta = 43$ and 52° , and the particle size (30 nm) was determined by the Debye–Scherrer equation. The transmission electron microscopy analysis revealed a spherical-shaped particle with an average size of 20 nm. The EDX analysis of the as-synthesized CuNPs revealed the presence of the element Cu, which was not present in the EDX image of the biofloculant used in the synthesis of the CuNPs; this indicated the success of biosynthesis.



Citation: Tsilo, P.H.; Basson, A.K.; Ntombela, Z.G.; Dlamini, N.G.; Pullabhotla, R.V.S.R. Biosynthesis and Characterization of Copper Nanoparticles Using a Biofloculant Produced by a Yeast *Pichia kudriavzevii* Isolated from Kombucha Tea SCOBY. *Appl. Nano* **2023**, *4*, 226–239. <https://doi.org/10.3390/applnano4030013>

Academic Editors: Anthony William Coleman and Giacomo Dacarro

Received: 16 March 2023

Revised: 31 July 2023

Accepted: 7 August 2023

Published: 11 August 2023



Copyright: © 2023 by the authors. Licensee MDPI, Basel, Switzerland. This article is an open access article distributed under the terms and conditions of the Creative Commons Attribution (CC BY) license (<https://creativecommons.org/licenses/by/4.0/>).

Keywords: copper nanoparticles; *Pichia kudriavzevii*; Kombucha tea SCOBY; biofloculant; biosynthesis; characterization

1. Introduction

Nanoparticles have been studied in several branches of study, including chemistry, physics, medicine, biology, material science, and pharmacy. This is due to their unique optical and electrical properties that distinguish them from their bulk counter parts [1,2]. Nanomaterials are defined as elements with a dimension of 1 to 100 nanometers. The characteristics of nanoparticles are improved as their size is reduced [3]. These characteristics include increased surface area, enhanced surface reactivity, improved mechanical properties, altered optical and electronic properties, enhanced bioavailability, and cellular uptake. The major strength of nanomaterials to be used in various applications is determined by their physical and chemical features [4]. Nanoparticles can be used to provide new, cutting-edge applications in energy storage [5], optics [6], sensing [6], communications [7],

data storage [8], biology and medicine [9], transmission [10], and environmental protection, among other fields [11]. Moreover, in recent years, major attempts have been made to generate a large number of nanoparticles/nanocrystals with regulated morphologies, sizes, and forms [12]. Copper, titanium, manganese, gold, silver, iron, tantalum, aluminium, or a combination of at least two of these nanoparticles are some of the nanoparticles being investigated [13].

Copper nanoparticles have gained researchers' interest in recent years because of their attributes such as in-expensive production costs and antibacterial efficacy [14]. Nanoparticles have a high surface area to volume ratio, catalytic activity, magnetic properties, and optical properties when compared to precious metals such as gold, palladium, or silver [15]. Nevertheless, when exposed to air, their quick oxidation becomes the most difficult aspect of their preparation and storage. Scientists have used innocuous media such as argon and nitrogen to resolve these challenges of oxidation [16]. Copper salt is also protected or rather capped using reducing agents from being further oxidized.

The reducing and capping compounds utilized in the synthesis of nanoparticles have been discovered to be hazardous and expensive [17]. Consequently, the use of a bioflocculant has been seen as a better alternative in the chemical reduction process to counteract the toxicity of chemicals used as reducing agents and to synthesize copper nanoparticles for a greener environment [16]. The bioflocculant in the process acts as a reducing and a capping agent, making the procedure non-toxic, environmentally benign, and cost effective as bioflocculants are non-toxic. Several metallic and non-metallic nanoparticles have been in an increased demand in recent years owing to their fascinating characteristics [18].

Lee et al. [19] successfully produced stable copper nanoparticles (CuNPs) by treating an aqueous solution of copper sulfate pentahydrate with an extract derived from *Magnolia kobus* leaves. Stable copper nanoparticles were synthesized through a green approach utilizing *Ocimum sanctum* leaf extract, as developed by Kulkarni and Kulkarni [20]. CuNPs were biosynthesized by Varshney et al. [21] utilizing a *Pseudomonas stutzeri* bacterial strain isolated from wastewater originating from the electroplating industry.

Nanoparticles of various sizes, compositions, and forms have been synthesized by utilizing a variety of processes [15]. Physical and chemical processes are utilized in these treatments of nanoparticles synthesis. Laser ablation and high-energy irradiation techniques are utilized in physical procedures. Chemical procedures utilizing reducing agents are part of the chemical approach to the synthesis of nanoparticles [16]. Although chemical and physical methods are frequently used to generate nanoparticles, they are not only expensive but also damaging to the environment and living things [22]. The widespread usage of the produced products (bio-materials) necessitates significant energy use, the use of hazardous organic solvents, the production of new disposal intermediates, and, eventually, biological risks and environmental degradation [23]. Thus, in this paper we report the biosynthesis of copper nanoparticles using a bioflocculant produced by a yeast *Pichia kudriavzevii* as a stabilizing and capping agent and their characterization using various methods such as Fourier transform infrared spectroscopy (FT-IR), X-ray diffraction pattern (XRD), transmission electron microscopy (TEM), ultraviolet visible microscopy (UV-Vis), scanning electron microscopy (SEM), and energy dispersive X-ray analysis (EDX).

2. Materials and Methods

2.1. Bioflocculant Source and Production Medium

The bioflocculant was produced from a yeast *Pichia kudriavzevii*, which was isolated from Kombucha tea SCOBY and identified as *Pichia kudriavzevii* MH545928.1 by using the 16S rRNA technique as described by Tsilo et al. [24]. The method outlined by Shukri [25] was followed to compose a bioflocculant production medium. The medium consisted of 1 L Kombucha tea broth, glucose (20 g), $MgSO_4 \cdot 7H_2O$ (0.2 g), $(NH_4)_2SO_4$ (0.2 g), K_2HPO_4 (5 g), urea (0.5 g), yeast extract (0.5 g), and KH_2PO_4 (2 g) at pH 7 and was autoclaved at 121 °C for 15 min for sterility. After autoclaving, the medium was allowed to cool down

before being inoculated with a fresh culture (revived overnight), and it was incubated for 60 h at 35 °C with agitation of 140 rpm in a shaker incubator.

2.2. Extraction and Purification of the Bioflocculant

Following 60 h of fermentation at 35 °C, the broth culture was removed and centrifuged for 15 min at 8000 rpm and at 4 °C. This was performed to separate the cells and insoluble substances before transferring the suspension to a clean beaker and discarding the sediment cells. Thereafter, 1 L of distilled water was added to the clear suspension, which was then re-centrifuged at 8000 rpm for 15 min at 4 °C. The solution was shaken and left to stand at 4 °C for 12 h after 2 volumes of ice-cold ethanol was added to the suspension. A precipitate was collected and vacuum-dried before being mixed with 100 mL of distilled water and the combination of chloroform and n-butyl alcohol (5:2 *v/v*). The mixture was allowed to stand at room temperature for 12 h. Thereafter, the precipitate was vacuum-dried to obtain a pure bioflocculant [26].

2.3. Synthesis of Copper Nanoparticles

A 200 mL solution of 3 mM copper sulphate was prepared with distilled water. Then, a 0.5 g of purified bioflocculant was added and the mixture was agitated for 10 min at room temperature in the shaking incubator at a speed of 200 rpm. The mixture was kept at room temperature for 24 h, and the precipitate was collected by centrifugation at 8000 rpm for 15 min at 4 °C. The visual observation of a color change from colorless to blue confirmed the synthesis of the CuNPs. The characterization of the as-synthesized material using various analytical techniques also confirms the formation of copper nanoparticles. A copper sulphate solution without bioflocculant was utilized as a control [26]. The vacuum-dried nanoparticles were kept in a safe place for further analysis.

2.4. Characterization of the Biosynthesized Copper Nanoparticles

The optical measurements of the produced copper nanoparticles and the bioflocculant were performed utilizing a Varian Cary 50 Conc. UV-Vis spectrophotometer (Orion AquaMate AQ8100, Gauteng, South Africa), with 0.1 mL of the sample diluted with 2 mL of distilled water. Quartz cuvettes were utilized to hold samples of about 1 cm path length. The absorption measurements were carried out in the wavelength range between 200–700 nm, with a resolution of 1 nm at room temperature.

The functional groups present in the bioflocculant, and the biosynthesized copper nanoparticles were identified and confirmed by utilizing a Fourier transform-infrared (FT-IR) Tensor 27 spectrophotometer (Bruker, Gauteng, South Africa) as part of the structural characterization. Pure solid materials were dried and crushed to a fine powder for FT-IR measurements, and the spectra were recorded using a Tensor 27 Bruker FT-IR spectrophotometer with a resolution of 4 cm⁻¹ in the 4000 to 400 cm⁻¹ range.

The X-ray diffraction (XRD) pattern was utilized to investigate the crystallinity of the dried copper nanoparticles. The patterns were recorded utilizing a Bruker D8 Advance diffractometer (Bruker, Gauteng, South Africa) equipped with Cu K α 1 radiation ($\lambda = 1.54060 \text{ \AA}$) at 40 kV/40 mA at ambient temperature. The dried sample was put on a flat sample holder and scanned in increments of 0.05 in a 0.003/s scan rate with a step size of 0.00657 between 5 and 90 °C.

The TEM micrographs were obtained using a JEOL 1010 transmission electron microscope (JEOL USA, Inc., Peabody, MA 01960, USA). By dabbing a drop of the diluted material onto the copper grid (150 mesh size), the specimens were made. At 100 kV accelerating voltage, the samples were observed, and a Magaview III camera was used to take digital images.

At 1000 keV/wavelengths of resolution, scanning electron microscopy (SEM-Sipma-VP-03-67, Johannesburg, South Africa) was utilized to provide a better image and the elements of both the bioflocculant and biosynthesized CuNPs. Using a PerkinElmer Thermal Analysis Pyris 6 TGA, thermogravimetric analysis measurements were taken

on the copper nanoparticles as they were being synthesized (PerkinElmer, Inc., Waltham, MA 02451, USA). The temperature ramped up from 22 to 900 °C at a rate of 10 °C/min while the nitrogen gas flow rate was kept constant at 40 cc/min (Dlamini et al., 2019).

3. Results

3.1. FT-IR Analysis

Microorganisms produce biofloculants with varying chemical compositions [24]. The flocculating action of a produced biofloculant is exclusively determined by its chemical makeup, which is linked to the functional groups in the molecule. The functional groups in the molecule also act as a binding site for distinct colloids in solution [25]. The Fourier transform infrared (FT-IR) spectroscopy investigation revealed various functional groups present in the molecule. The FT-IR spectra of the biofloculant and biosynthesized copper nanoparticles' functional groups are shown in Figure 1. The figure showed the characteristic peak at 3267 cm^{-1} (-OH), 2956 cm^{-1} (O-H), 1656 cm^{-1} (C=C), 1059 cm^{-1} (C-N), and 511 cm^{-1} (C-I), which represents the different functional groups (hydroxyl, carboxylic acid, alkenes, amine, and halo compounds, respectively) present in the bio-floculant. The characteristic peaks at band values of 3482 cm^{-1} (-OH), 3261 cm^{-1} (-OH), 1640 cm^{-1} (C=C), 1059 cm^{-1} (C-O), 580 cm^{-1} (C-Br), and 519 cm^{-1} (C-Br) showed the functional groups (hydroxyl, alkene, alcohol, and halo compounds, respectively) available in the as-synthesized copper nanoparticles. The band at 3267 cm^{-1} for the biofloculant and those around 3482 and 3261 cm^{-1} for the CuNPs represent hydroxyl (-OH) groups and amine (-NH₂) groups, respectively. These peaks have been reported to reduce Cu²⁺ to Cu⁰ [26]. The stretching vibration between 1059 cm^{-1} and 519 cm^{-1} could be assigned to the copper oxide bond in the as-prepared copper nanoparticles [27]. The study findings from the FT-IR spectra supported the hypothesis that the produced nanoparticles were coated with biomolecules that were in charge of reducing the copper oxide ions and protecting the nanoparticles in the biosynthesis of CuNPs [28]. An FT-IR analysis of CuNPs in a study by Harne et al. [29] demonstrated a prominent absorption band at 1610 cm^{-1} by a *Calotropis procera* L., which could be assigned to the binding of -NH-C=O to metal (copper) nanoparticles. They further reported additional important FT-IR bands at 2916, 1510, 1230, 1321, and 1027 cm^{-1} , which all supported the formation of CuNPs. Another study by Saranyaadevi et al. [30] revealed peaks at 3901, 3840, 3842, 3460, and 1636 cm^{-1} in the FT-IR spectra. These results agree with those of the present study.

3.2. UV-Visible Spectroscopy Analysis

The UV-visible spectra of the biofloculant and biosynthesized copper nanoparticles are shown in Figure 2. The surface plasmon resonance (SPR) spectra with absorption peaks between 200–350 nm were observed in the biofloculant (Figure 2). The biofloculant was revealed to have a sharp peak at around 250 nm. The peak maxima for the biosynthesized Cu nanoparticles were observed at 555 nm and 575 nm, which could be attributed to the copper nanoparticles. An SPR peak at around 553 nm was reported for bimetallic copper nanoparticles in a study by Punniyakotti et al. [27]. Rajesh et al. [28] documented CuNPs with surface plasmon resonance produced at 580 nm. The UV-vis spectra showed the Cu metal ion's SPR action, which caused the formation of the highest absorbance of nanoparticles at about 555 nm [29]. A study by Amaliyah et al. [30] reported UV-vis spectra with two peak maxima at around 203–210 nm (first peak) and 234–255 nm (second peak). During synthesis, the solution (biofloculant and 3 mM CuSO₄) the color changed from white to blue, thus indicating the formation of copper nanoparticles. The surface plasmon vibration in the copper nanoparticles caused them to turn blue in solution. The color shift indicated the reduction of Cu ions into CuNPs by adding aqueous leaf extract of *Cardiospermum halicacabum* (CH) as a green reducing agent in a study by Punniyakoti et al. [27], and this color change indicated the formation of CuNPs. The color change could also be attributed to the interaction of metal nanoparticles conducting electrons with incoming photons [31].

One can deduce from this analysis that there is a relationship between the biofloculant and the as-synthesized CuNPs as indicated by the peaks (Figure 2).

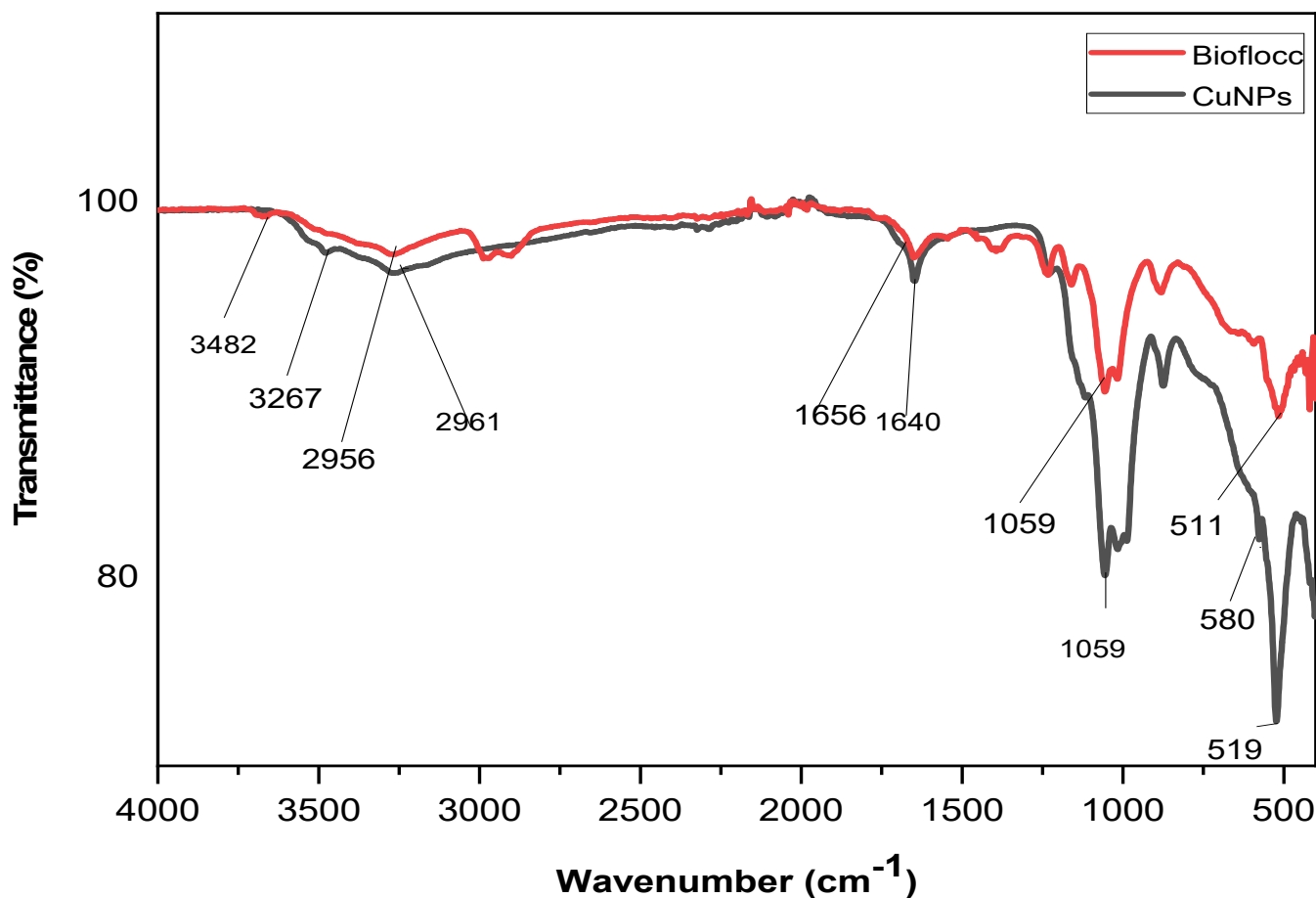


Figure 1. FT-IR spectra of the biofloculant and ss-synthesized copper nanoparticles.

3.3. X-ray Diffraction Patterns

The crystalline properties of the produced nanoparticles were determined by utilizing X-ray diffraction (XRD). The diffractogram of the biofloculant showed diffraction peaks at 2-theta equal to 20.1, 21.7, 24, 30.9, and 34.12°. When compared to the Cu nanoparticles, these peaks observed on a biofloculant may be the result of impurities present in the molecule (Dlamini, 2017).

The X-ray diffraction profile of the biosynthesized copper nanoparticles using a biofloculant as a passivating agent and the biofloculant are shown in Figure 3. These diffraction peaks identified in the XRD spectra correspond to the planes (200) and (220) at 2-theta values of 43° and 51°, respectively. The diffraction peak (200) was shown to have the highest intensity peak. Other small peaks were observed at 23° and 29.6° representing the (100) and (110) planes, respectively, indicating the presence of Cu₂O impurities in the as-synthesized Cu nanoparticles [32]. All of these peaks corresponded to the face centered cubic (FCC) structure and were in good agreement with the standard JCPDS No. 04-0836 cord [33]. The peak positions match those in the literature for metallic copper [34]. There were no further impurity-related peaks in the sample in relation to the JCPDS standards. Caroling et al. [35] reported the presence of Cu₂O in the XRD spectra of CuNPs when the PEG (polyethylene glycol) 600 capping agent was absent, but when it was used, there was no Cu₂O formed, so this meant that PEG 600 protected the synthesis of CuNPs from oxidation. However, in the present study, Cu₂O was observed from the XRD spectra which means that the CuNPs' formation was not well protected from oxidation. The crystallite size was estimated to be around 30 nm using Scherrer's equation. Similar results were

observed in a study by Akhter et al. [36] where they reported a crystallite size of above 30 nm for CuNPs using Scherrer's formula. Muthulakshmi et al. [37] observed similar results for the biosynthesis of CuNPs using a biofloculant from cellulose. Based on the XRD profile, it can be concluded that biofloculant from *Pichia kudriavzevii* can be utilized to synthesize pure copper nanoparticles.

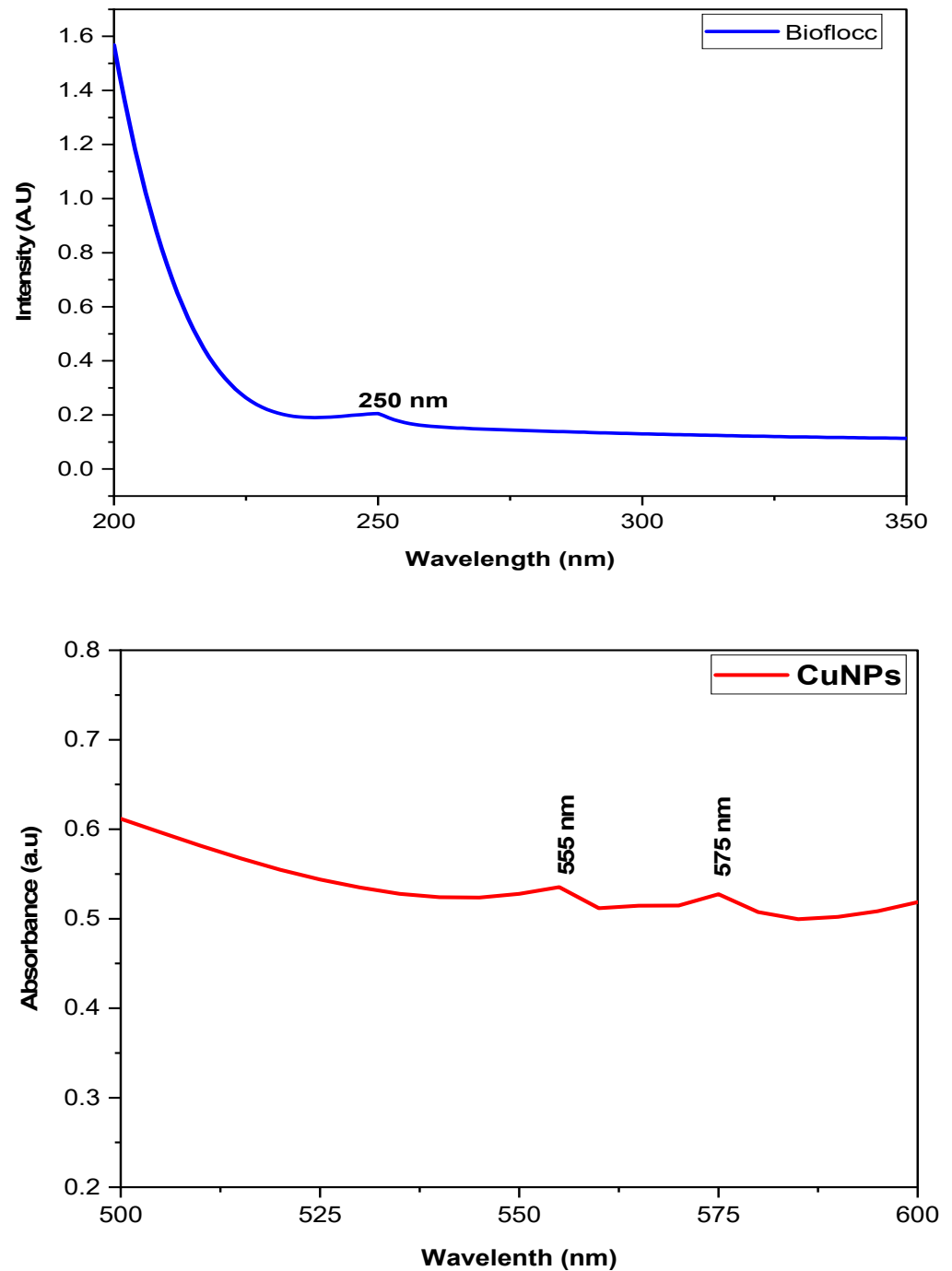


Figure 2. UV-visible spectra of the biofloculant and biosynthesized CuNPs.

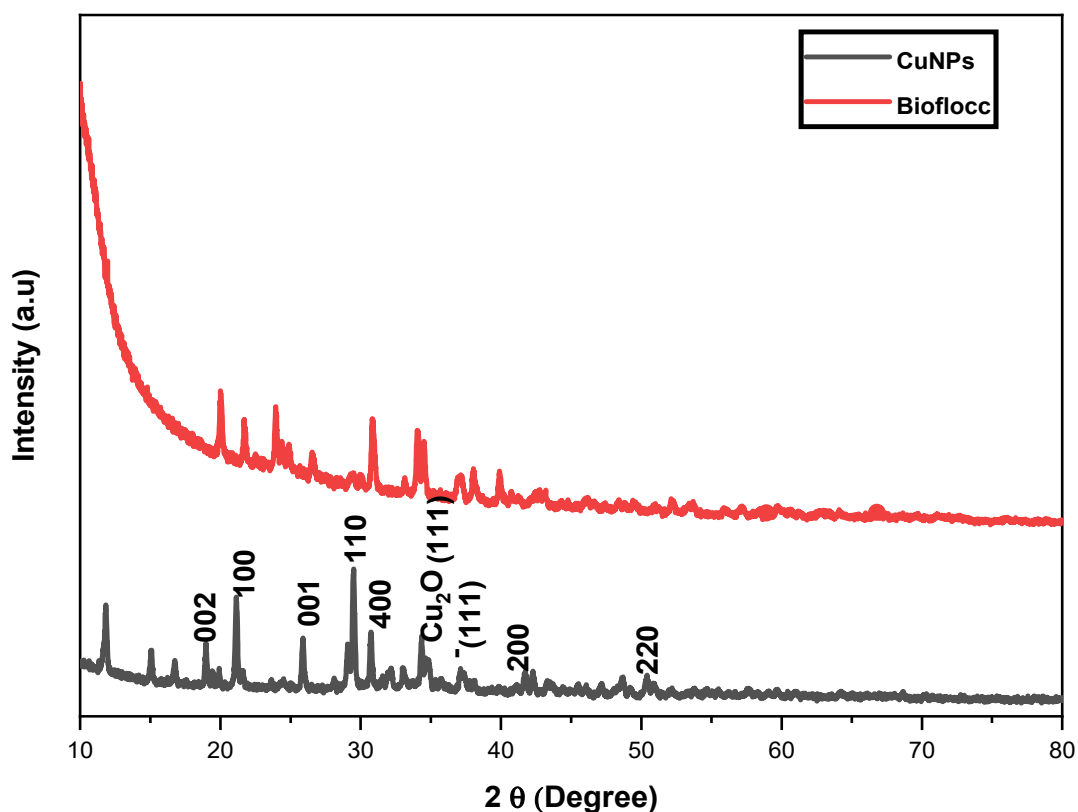


Figure 3. X-ray diffraction pattern of the biofloculant and the as-synthesized copper nanoparticles.

The Debye–Scherrer equation $D = \frac{K\lambda}{\beta \cos\theta}$ was used to calculate the average particle size of the CuNPs, where K is the Scherrer constant which is within the value of 0.9 to 1, D is the nanoparticles' crystallite size at full width half maximum (FWHM), λ (0.541 nm) is the wavelength of the X-ray used in the XRD, β is the full width at half maximum diffraction peak, and θ is the Bragg's angle.

3.4. TEM Analysis

The TEM image in Figure 4a shows the CuNPs that are agglomerated and are different from that of the biofloculant (Figure 4b) used for its preparation. The biofloculant showed particles that are rod-like and amorphous-mass-like, this cluster could be the reason behind the spherical shape observed on the biofloculant-passivated CuNPs after synthesis. It was observed that the synthesized Cu nanoparticles were spherical in shape. The effective biosynthesis of CuNPs was demonstrated by TEM images, with the average particle size estimated to be 20 nm, which was almost similar to the particle size obtained from the XRD pattern. The TEM histogram also showed the average particle size of 20 nm, and the graph was unimodal. The histogram was shown to be skewed to the left, indicating that there were smaller particles observed. These findings are in accordance with those reported by Sharma et al. [38], where TEM analysis was used to determine the shape of the synthesized copper nanoparticles and they were spherical in shape with small diameters. Amer and Awwad [39] reported CuNP nanoparticles with an average particle size of 18 nm using TEM analysis. While in other study by Chandra et al. [40], the TEM micrograph revealed particles with spherical morphology and a size range of 15 nm. The idea that the biofloculant acts as a capping agent to obtain the dominating fashioning of spherical CuNPs is supported by these data [41].

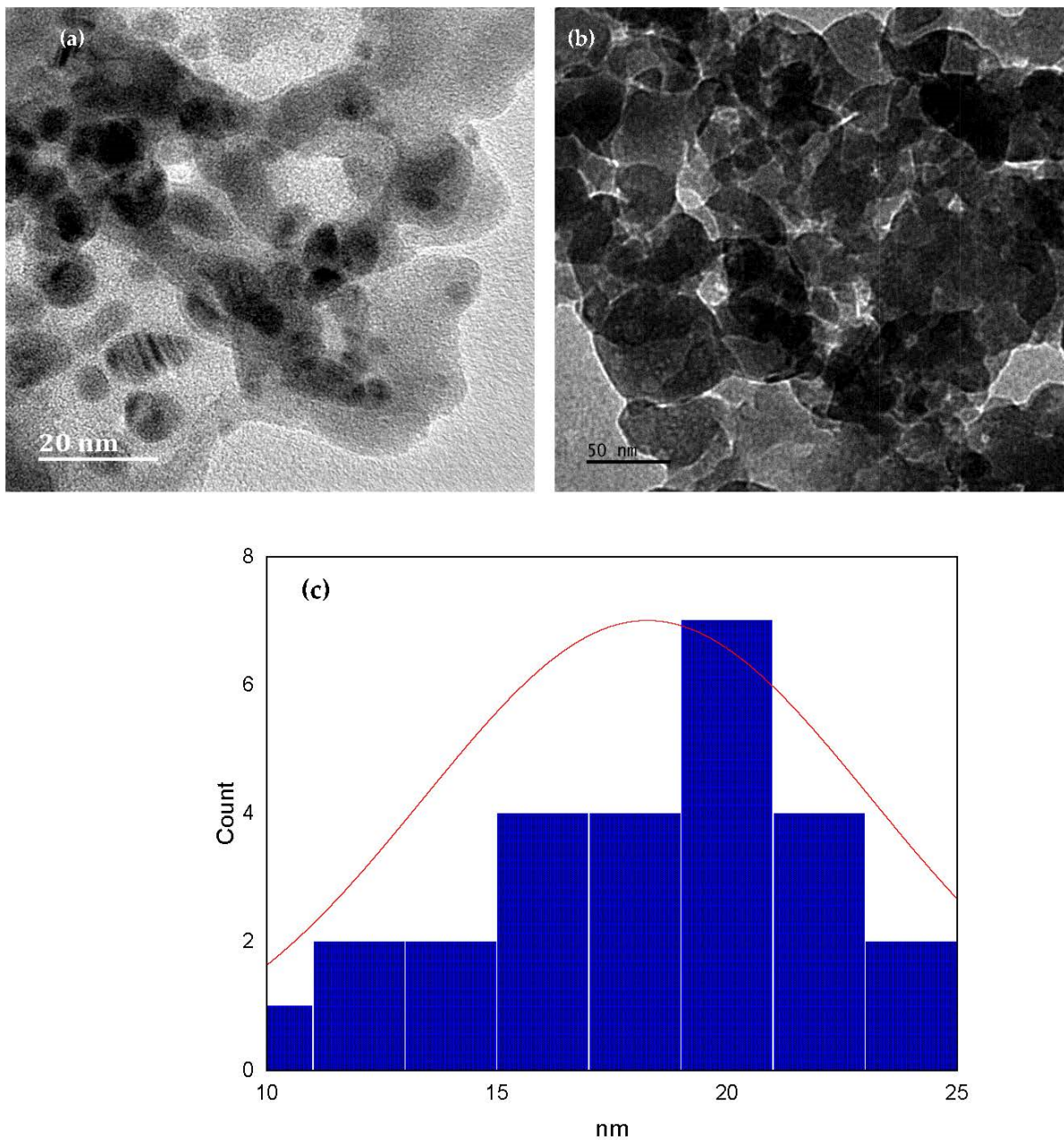


Figure 4. TEM images of (a) the copper nanoparticles, (b) the biofloculant, and (c) the particle size distribution histogram.

3.5. Thermogravimetric Analysis

The biosynthesized copper nanoparticles were subjected to thermogravimetric analysis to see how they react to extremely high temperatures. Figure 5 shows the results of a study on the thermal behavior of copper nanoparticles as a function of percentage weight residues at increasing temperatures between 24 and 900 °C in comparison to that of a biofloculant used for their preparation. It was discovered that there were three phases to the breakdown of the copper nanoparticles. The weight loss in the first phase (24–102 °C) corresponds to the loss of water and any other volatile substances. The weight loss for the copper nanoparticles was discovered to be 2.55% within this range, and for the biofloculant, it was 3.69%. In the case of modified copper sulphate, it reflects a minor reduction in water absorption because of the in situ biosynthesized CuNPs. The copper NPs and biofloculant composites were shown to have less thermal stability in the second phase (99–205 °C). The organic material that was present in both the copper nanoparticles and the biofloculant

may have degraded throughout this phase. The weight loss at this stage was 19.54 wt% for both samples. Similar findings were made when *Ocimum sanctum* leaf extract was used as a reducing agent in the case of cellulose nanocomposite films containing in-situ-produced CuNPs [42]. The biosynthesized CuNPs lost about 10.6% of their weight in the third stage (205–895 °C), which was a higher temperature. However, it could be noted that the weight loss (17.5%) of the bioflocculant was higher at higher temperatures (205–895 °C) compared to that of the CuNPs (10.6%). This could be because of the bioflocculant being used during synthesis as a stabilizing and protecting agent for the CuNPs. The bioflocculant used in CuNP synthesis was previously reported to be thermally stable [24].

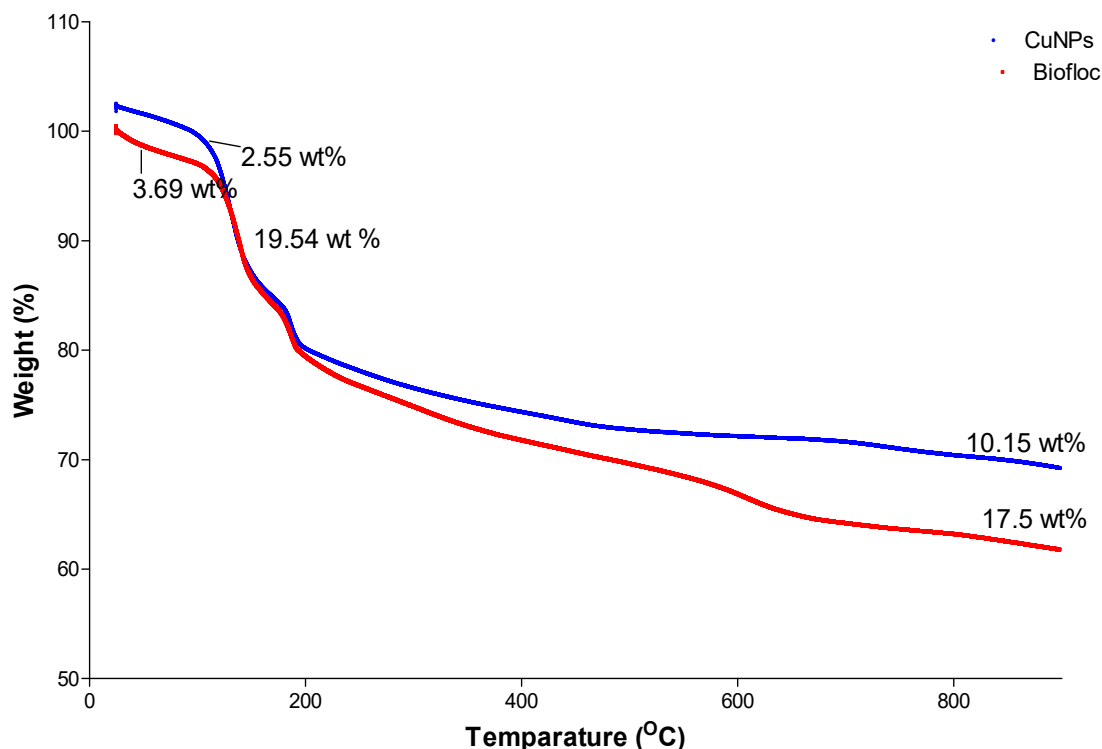


Figure 5. TG analysis of the bioflocculant and copper nanoparticles.

The combination of sugars and amino acid components was discovered, as revealed by the FT-IR analysis, suggesting that the biosynthesized CuNPs have thermo-labile and thermostable contents. The first weight loss may have been caused by the evaporation or surface absorbance of both moisture and water or it may have been due to the presence of C=O and -OH functional groups in the molecular chain of the bioflocculant/copper nanomaterials formed in the presence of a bioflocculant. Ashok et al. [43] reported similar findings with three stages of thermal degradation of CuNPs. In another study by Prabhu et al. [44], it was reported that the sample's carbonaceous matter was dissipated in the third stage, which had a weight loss of 0.881% between 550 and 800 °C. This affirmed our study's findings whereby 10.6% weight loss was reported for temperatures above 205 °C.

3.6. SEM Analysis

The biosynthesized CuNPs were discovered to be irregular in shape, primarily in the form of polygons, squares, and some spherical particles in clusters and aggregated in smaller clusters, as shown by the SEM image (Figure 6a). The bioflocculant's cumulus-like shape is demonstrated in Figure 6b. This make-up of the bioflocculant enabled the biosynthesis of the CuNPs. The formation of CuNPs by the bioflocculant is attributed to electrostatic interactions and hydrogen bonds between the bio-organic capping molecules [45]. These nanoparticles' aggregation and amalgamation is a clear indication of their high surface energies [46]. It has been reported that the stability of nanocomposites and agglom-

eration are significantly impacted by ecological variables [47]. Consequently, throughout the generation of nanoparticles, they bind to one another and spontaneously form asymmetric clusters [48].

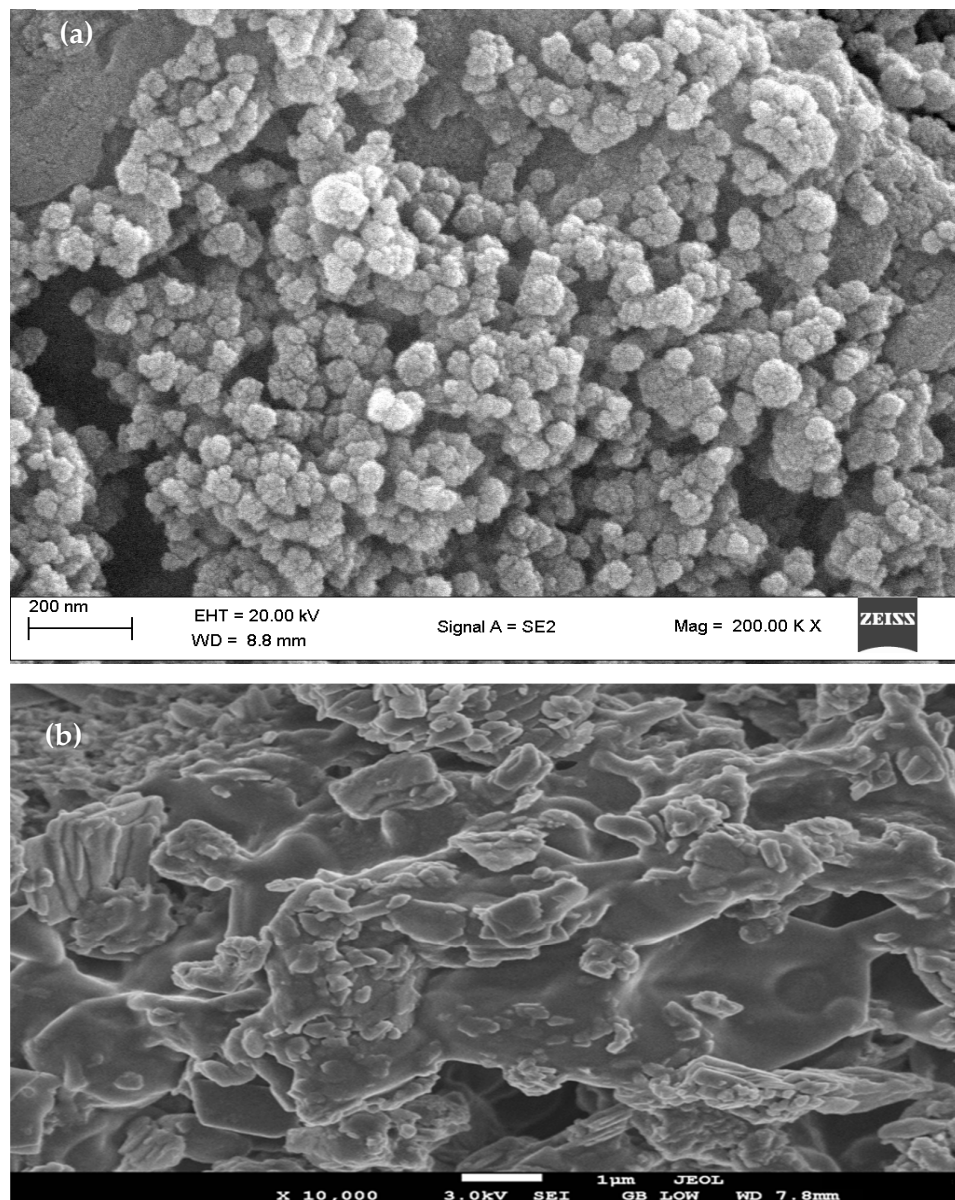
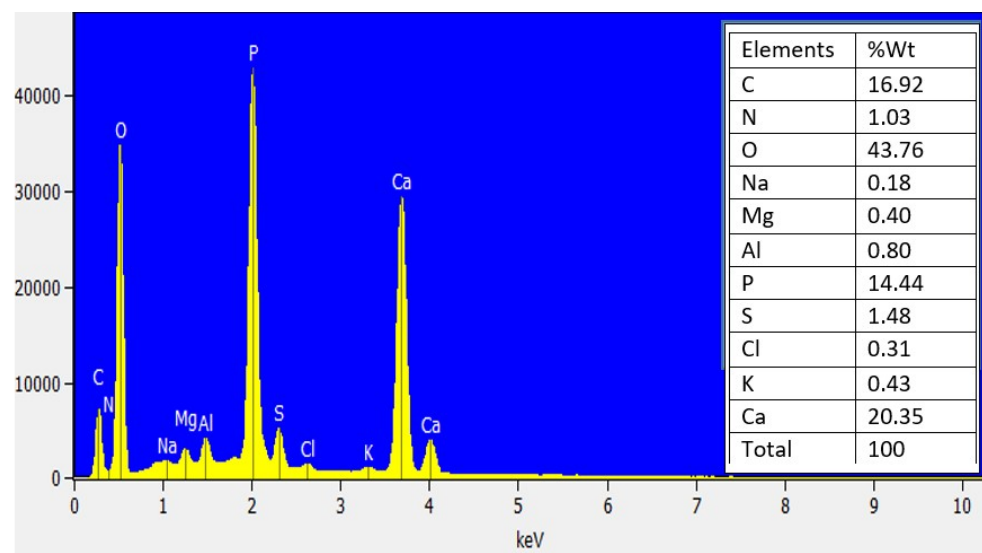


Figure 6. SEM images of (a) the biosynthesized CuNPs and (b) the biofloculant.

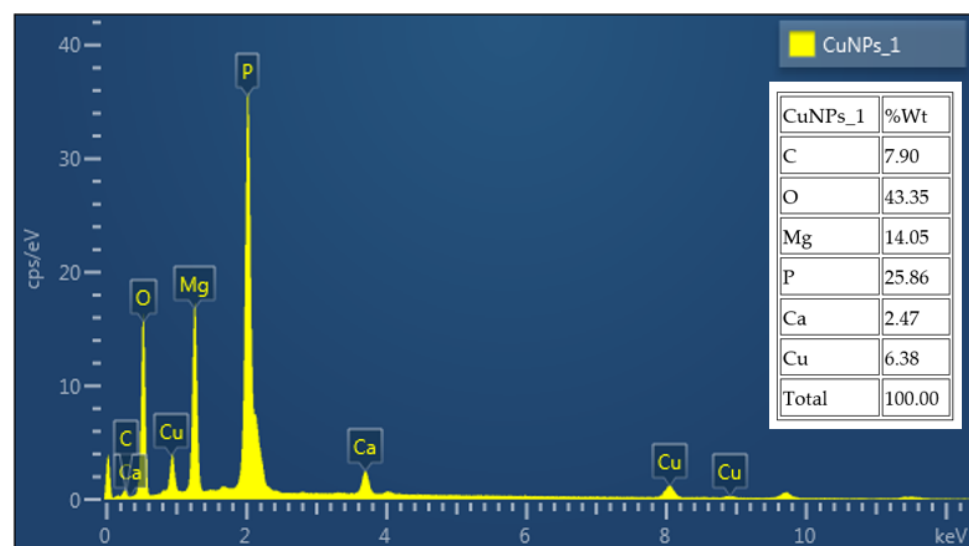
3.7. EDX Analysis

The purified biofloculant and biosynthesized copper nanoparticles contain several different elements, as shown by the SEM-EDX data (Figure 7). The copper metallic nano-materials are responsible for the significant peak at 1 keV seen in the EDX analysis of the generated copper nanoparticles (Figure 7b) [49]. The spectra also showed the presence of additional peaks with N, O, Mg, P, Ca, and Cu (around 8 and 9 keV) properties. In actuality, these elements came from the phytochemicals in the green tea used to prepare Kombucha tea [50]. These substances confirm once more that the biosynthesized nanoparticles were coated with the examined organic bio-matter. The EDX spectrum of the biofloculant (Figure 7a) showed important elements such as carbon, nitrogen, and oxygen, among others, of which the biofloculant was mainly composed, confirming it to be a polysaccharide. Other elements such as the existence of Cu (Figure 7b) affirmed that copper

nanoparticles were successfully synthesized as copper was not present in the EDX of the purified biofloculant. This, therefore, signifies the successful biosynthesis of CuNPs. In a study by Suarez-Cerda et al. [51], EDX examination revealed a signal which indicated there was substantial copper present but no oxygen, proving that metallic copper Cu-NPs were biosynthesized. While in another study by Asghar and Asghar [52], it was reported that, Cu signals with high specificity and strength were generated by the SPR and occurred at 8.04 and 0.93 keV for $L\alpha$ and $K\alpha$ nanoparticles, respectively. Due to the biomolecules from the plant that were bonded to the surface of the nanoparticles, the signal for C and O was also produced. Additionally, at around 3.69, 2.30, 1.74, 1.48, and 1.04 keV, the EDX patterns also revealed a few meager hints of Ca, S, Si, Al, and Na, respectively. The high levels of phosphorus on the EDX of the biosynthesized CuNPs could be the result of a biofloculant used as a coating agent. There was about 14.44% wt of phosphorus on the structure of the biofloculant used for synthesis; in the CuNPs' EDX patterns, P could also be the cause of unintended side reactions leading to the incorporation of phosphorus species.



(a)



(b)

Figure 7. Energy-dispersive X-ray spectra of (a) the purified biofloculant and (b) the as-synthesized copper nanoparticles.

4. Conclusions

The purified bioflocculant from *Pichia kudriavzevii* was successfully utilized in the synthesis of copper nanoparticles, and the procedure proved to be quick, easy, and environmentally benign because it uses a bioflocculant which can be easily biodegraded. Characterization of the copper nanoparticles through FT-IR revealed the presence of some useful functional groups such as hydroxyl groups, amines, and CuO. The FT-IR also showed some similar functional groups between the bioflocculant and the copper nanoparticles such as -OH, NH₂, and COOH. The UV-visible spectrum of the biosynthesized CuNPs showed the peak maxima at absorbance between 200–700 nm which confirms the formation of CuNPs. The TEM images indicated that the produced nanoparticles are close to spherical in shape with an average particle size of 20 nm which was also confirmed using Scherrer's equation. The SEM-EDX results of the CuNPs showed elements such as C, O, Mg, P, Ca, and Cu with their weight percentages (wt%). Cu was present with 6.8%wt, showing that the bioflocculant used was able to act as a reducing and capping agent during synthesis.

Author Contributions: Conceptualization, R.V.S.R.P. and Z.G.N.; methodology, P.H.T.; software, P.H.T.; validation, Z.G.N. and N.G.D.; formal analysis, P.H.T.; investigation, P.H.T.; resources, R.V.S.R.P.; data curation, P.H.T.; writing—original draft preparation, P.H.T.; writing—review and editing, Z.G.N., N.G.D. and R.V.S.R.P.; supervision, Z.G.N., N.G.D., A.K.B. and R.V.S.R.P. All authors have read and agreed to the published version of the manuscript.

Funding: This research was funded by the National Research Foundation (NRF, South Africa) in the form of the Incentive Fund Grant (grant no. 103691) and the Research Developmental Grant for Rated Researchers (112145) and the Council for Scientific and Industrial Research's (CSIR).

Data Availability Statement: Data is not available on online platforms. However, once the thesis is approved, it will be available through the Institutions Library repository.

Acknowledgments: The authors would like to acknowledge the University of KwaZulu-Natal Microscopy and Microanalysis Unit for providing support by letting us use the TEM and SEM-EDX facilities for the characterization of the nanomaterials. Rajasekhar Pullabhotla would like to acknowledge the National Research Foundation (NRF, South Africa) for their financial support in the form of the Incentive Fund Grant (grant no. 103691) and the Research Developmental Grant for Rated Researchers (112145). Phakamani Tsilo would like to acknowledge the Council for Scientific and Industrial Research (CSIR, South Africa) for the financial assistance provided in the form of a Ph.D. bursary.

Conflicts of Interest: The authors declare no conflict of interest.

References

1. El-Zahed, M.M.; Baka, Z.A.; El-Sayed, A.K.; Abou-Dobara, M.I. The Anti-Aspergillus Potential of Optimized Biosynthesized Reduced Graphene Oxide/Silver Nanocomposite Using *Escherichia Coli* D8 (Mf062579). *J. Microbiol. Biotechnol. Food Sci.* **2022**, *12*, e5864. [[CrossRef](#)]
2. Mughal, S.S.; Hassan, S.M. Comparative study of AgO nanoparticles synthesize via biological, chemical and physical methods: A review. *Am. J. Mater. Synth. Process.* **2022**, *7*, 15–28.
3. Tian, T.; Ruan, J.; Zhang, J.; Zhao, C.-X.; Chen, D.; Shan, J. Nanocarrier-based tumor-targeting drug delivery systems for hepatocellular carcinoma treatments: Enhanced therapeutic efficacy and reduced drug toxicity. *J. Biomed. Nanotechnol.* **2022**, *18*, 660–676. [[CrossRef](#)] [[PubMed](#)]
4. Ealia, S.A.M.; Saravanakumar, M. A review on the classification, characterisation, synthesis of nanoparticles and their application. in IOP conference series: Materials science and engineering. *IOP Conf. Ser. Mater. Sci. Eng.* **2017**, *263*, 032019. [[CrossRef](#)]
5. Khan, K.; Tareen, A.K.; Aslam, M.; Mahmood, A.; Zhang, Y.; Ouyang, Z.; Guo, Z.; Zhang, H. Going green with batteries and supercapacitor: Two dimensional materials and their nanocomposites based energy storage applications. *Prog. Solid State Chem.* **2020**, *58*, 100254. [[CrossRef](#)]
6. Pal, K.; Si, A.; El-Sayyad, G.S.; Elkodous, M.A.; Kumar, R.; El-Batal, A.I.; Kralj, S.; Thomas, S. Cutting edge development on graphene derivatives modified by liquid crystal and CdS/TiO₂ hybrid matrix: Optoelectronics and biotechnological aspects. *Crit. Rev. Solid State Mater. Sci.* **2021**, *46*, 385–449. [[CrossRef](#)]
7. Godara, S.; Mahato, P. Potential applications of hybrid nanocomposites. *Mater. Today Proc.* **2019**, *18*, 5327–5331. [[CrossRef](#)]
8. Okpala, C.C. Nanocomposites—An overview. *Int. J. Eng. Res. Dev.* **2013**, *8*, 17–23.

9. Koo, J.H. *Polymer Nanocomposites: Processing, Characterization, and Applications*; McGraw-Hill Education: New York, NY, USA, 2019.
10. Wu, W.; Chen, W.; Yang, S.; Lin, Y.; Zhang, S.; Cho, T.-Y.; Lee, G.; Kwon, S.-C. Design of AlCrSiN multilayers and nanocomposite coating for HSS cutting tools. *Appl. Surf. Sci.* **2015**, *351*, 803–810. [[CrossRef](#)]
11. Singh, K.R.; Solanki, P.R.; Malhotra, B.; Pandey, A.C.; Singh, R.P. Introduction to nanomaterials: An overview toward broad-spectrum. In *Applications*; CRC Press: Boca Raton, FL, USA, 2021.
12. Younis, A.; Chu, D.; Kaneti, Y.V.; Li, S. Tuning the surface oxygen concentration of {111} surrounded ceria nanocrystals for enhanced photocatalytic activities. *Nanoscale* **2016**, *8*, 378–387. [[CrossRef](#)] [[PubMed](#)]
13. Lalis, A.; Tessier, G.; Plain, J.; Baffou, G. Quantifying the efficiency of plasmonic materials for near-field enhancement and photothermal conversion. *J. Phys. Chem. C* **2015**, *119*, 25518–25528. [[CrossRef](#)]
14. Kamanna, K.; Amaregouda, Y. Synthesis of bioactive scaffolds catalyzed by agro-waste-based solvent medium. *Phys. Sci. Rev.* **2022**. [[CrossRef](#)]
15. Ahmed, E.; Kalathil, S.; Shi, L.; Alharbi, O.; Wang, P. Synthesis of ultra-small platinum, palladium and gold nanoparticles by *Shewanella loihica* PV-4 electrochemically active biofilms and their enhanced catalytic activities. *J. Saudi Chem. Soc.* **2018**, *22*, 919–929. [[CrossRef](#)]
16. Tijani, J.O.; Fatoba, O.O.; Madzivire, G.; Petrik, L.F. A review of combined advanced oxidation technologies for the removal of organic pollutants from water. *Water Air Soil Pollut.* **2014**, *225*, 1–30. [[CrossRef](#)]
17. Khodadadi, B.; Bordbar, M.; Nasrollahzadeh, M. Green synthesis of Pd nanoparticles at Apricot kernel shell substrate using *Salvia hydrangea* extract: Catalytic activity for reduction of organic dyes. *J. Colloid Interface Sci.* **2017**, *490*, 1–10. [[CrossRef](#)]
18. Owaid, M.N.; Ibraheem, I.J. Mycosynthesis of nanoparticles using edible and medicinal mushrooms. *Eur. J. Nanomed.* **2017**, *9*, 5–23. [[CrossRef](#)]
19. Lee, H.J.; Song, J.Y.; Kim, B.S. Biological synthesis of copper nanoparticles using *Magnolia kobus* leaf extract and their antibacterial activity. *J. Chem. Technol. Biotechnol.* **2013**, *88*, 1971–1977.
20. Kulkarni, V.D.; Kulkarni, P.S. Green synthesis of copper nanoparticles using *Ocimum sanctum* leaf extract. *Int. J. Chem. Stud.* **2013**, *1*, 1–4.
21. Varshney, R.; Bhadauria, S.; Gaur, M.; Pasricha, R. Copper nanoparticles synthesis from electroplating industry effluent. *Nano Biomed. Eng.* **2011**, *3*, 115–119. [[CrossRef](#)]
22. Marouzi, S.; Sabouri, Z.; Darroudi, M. Greener synthesis and medical applications of metal oxide nanoparticles. *Ceram. Int.* **2021**, *47*, 19632–19650. [[CrossRef](#)]
23. Shavandi, A.; Saeedi, P.; Ali, M.A.; Jalalvandi, E. Green synthesis of polysaccharide-based inorganic nanoparticles and biomedical aspects. In *Functional Polysaccharides for Biomedical Applications*; Elsevier: Amsterdam, The Netherlands, 2019; pp. 267–304.
24. Tsilo, P.H.; Basson, A.K.; Ntombela, Z.G.; Maliehe, T.S.; Pullabhotla, R.V. Isolation and optimization of culture conditions of a bioflocculant-producing fungi from Kombucha tea SCOBY. *Microbiol. Res.* **2021**, *12*, 950–966. [[CrossRef](#)]
25. Shukri, Z.N.A.; Chik, C.E.N.C.E.; Hossain, S.; Othman, R.; Endut, A.; Lananan, F.; Terkula, I.B.; Kamaruzzan, A.S.; Rahim, A.I.A.; Draman, A.S. A novel study on the effectiveness of bioflocculant-producing bacteria *Bacillus enclensis*, isolated from biofloc-based system as a biodegrader in microplastic pollution. *Chemosphere* **2022**, *308 Pt 2*, 136410. [[CrossRef](#)]
26. Dlamini, N.G.; Basson, A.K.; Pullabhotla, V.S.R. Optimization and application of bioflocculant passivated copper nanoparticles in the wastewater treatment. *Int. J. Environ. Res. Public Health* **2019**, *16*, 2185. [[CrossRef](#)] [[PubMed](#)]
27. Punniyakotti, P.; Panneerselvam, P.; Perumal, D.; Aruliah, R.; Angaiah, S. Anti-bacterial and anti-biofilm properties of green synthesized copper nanoparticles from *Cardiospermum halicacabum* leaf extract. *Bioprocess Biosyst. Eng.* **2020**, *43*, 1649–1657. [[CrossRef](#)] [[PubMed](#)]
28. Rajesh, K.; Ajitha, B.; Reddy, Y.A.K.; Suneetha, Y.; Reddy, P.S. Assisted green synthesis of copper nanoparticles using *Syzygium aromaticum* bud extract: Physical, optical and antimicrobial properties. *Optik* **2018**, *154*, 593–600. [[CrossRef](#)]
29. Nasrollahzadeh, M.; Momeni, S.S.; Sajadi, S.M. Green synthesis of copper nanoparticles using *Plantago asiatica* leaf extract and their application for the cyanation of aldehydes using $K_4Fe(CN)_6$. *J. Colloid Interface Sci.* **2017**, *506*, 471–477. [[CrossRef](#)] [[PubMed](#)]
30. Amaliyah, S.; Pangesti, D.P.; Masruri, M.; Sabarudin, A.; Sumitro, S.B. Green synthesis and characterization of copper nanoparticles using *Piper retrofractum* Vahl extract as bioreductor and capping agent. *Heliyon* **2020**, *6*, e04636. [[CrossRef](#)] [[PubMed](#)]
31. Jana, J.; Ganguly, M.; Pal, T. Enlightening surface plasmon resonance effect of metal nanoparticles for practical spectroscopic application. *RSC Adv.* **2016**, *6*, 86174–86211. [[CrossRef](#)]
32. Nagar, N.; Devra, V. Green synthesis and characterization of copper nanoparticles using *Azadirachta indica* leaves. *Mater. Chem. Phys.* **2018**, *213*, 44–51. [[CrossRef](#)]
33. Dlamini, N.G.; Basson, A.K.; Pullabhotla, V.S.R. Biosynthesis of bioflocculant passivated copper nanoparticles, characterization and application. *Phys. Chem. Earth Parts A B C* **2020**, *118*, 102898. [[CrossRef](#)]
34. Ali Soomro, R.; Sherazi, S.T.H.; Memon, N.; Shah, M.R.; Kalwar, N.H.; Hallam, K.R.; Shah, A. Synthesis of air stable copper nanoparticles and their use in catalysis. *Adv. Mater. Lett.* **2014**, *5*, 191–198. [[CrossRef](#)]
35. Caroling, G.; Vinodhini, E.; Ranjitham, A.M.; Shanthi, P. Biosynthesis of copper nanoparticles using aqueous *Phyllanthus embilica* (Gooseberry) extract-characterisation and study of antimicrobial effects. *Int. J. Nano Chem.* **2015**, *1*, 53–63.
36. Akhter, G.; Khan, A.; Ali, S.G.; Khan, T.A.; Siddiqi, K.S.; Khan, H.M. Antibacterial and nematocidal properties of biosynthesized Cu nanoparticles using extract of holoparasitic plant. *SN Appl. Sci.* **2020**, *2*, 1–6. [[CrossRef](#)]

37. Muthulakshmi, L.; Rajalu, A.V.; Kaliaraj, G.S.; Siengchin, S.; Parameswaranpillai, J.; Saraswathi, R. Preparation of cellulose/copper nanoparticles bionanocomposite films using a bioflocculant polymer as reducing agent for antibacterial and anticorrosion applications. *Compos. Part B Eng.* **2019**, *175*, 107177. [[CrossRef](#)]
38. Sharma, P.; Pant, S.; Dave, V.; Tak, K.; Sadhu, V.; Reddy, K.R. Green synthesis and characterization of copper nanoparticles by *Tinospora cardifolia* to produce nature-friendly copper nano-coated fabric and their antimicrobial evaluation. *J. Microbiol. Methods* **2019**, *160*, 107–116. [[CrossRef](#)]
39. Amer, M.; Awwad, A. Green synthesis of copper nanoparticles by Citrus limon fruits extract, characterization and antibacterial activity. *Chem. Int.* **2021**, *7*, 1–8. [[CrossRef](#)]
40. Chandra, S.; Kumar, A.; Tomar, P.K. Synthesis and characterization of copper nanoparticles by reducing agent. *J. Saudi Chem. Soc.* **2014**, *18*, 149–153. [[CrossRef](#)]
41. Nunthavarawong, P.; Rangappa, S.M.; Siengchin, S.; Thoppil-Mathew, M. *Antimicrobial and Antiviral Materials: Polymers, Metals, Ceramics, and Applications*; CRC Press: Boca Raton, FL, USA, 2022.
42. Sadanand, V.; Rajini, N.; Rajulu, A.V.; Satyanarayana, B. Preparation of cellulose composites with in situ generated copper nanoparticles using leaf extract and their properties. *Carbohydr. Polym.* **2016**, *150*, 32–39. [[CrossRef](#)] [[PubMed](#)]
43. Ashok, B.; Hariram, N.; Siengchin, S.; Rajulu, A.V. Modification of tamarind fruit shell powder with in situ generated copper nanoparticles by single step hydrothermal method. *J. Bioresour. Bioprod.* **2020**, *5*, 180–185. [[CrossRef](#)]
44. Prabhu, Y.; Rao, K.V.; Sai, V.S.; Pavani, T. A facile biosynthesis of copper nanoparticles: A micro-structural and antibacterial activity investigation. *J. Saudi Chem. Soc.* **2017**, *21*, 180–185. [[CrossRef](#)]
45. Dlamini, N.G. *Biosynthesis of Copper Nanoparticles Using a Bioflocculant from Alcaligenis Faecalis, Characterization and Its Application*; University of Zululand: Empangeni, South Africa, 2017.
46. Ismail, M. Green synthesis and characterizations of copper nanoparticles. *Mater. Chem. Phys.* **2020**, *240*, 122283. [[CrossRef](#)]
47. Njuguna, J.; Ansari, F.; Sachse, S.; Rodriguez, V.M.; Siqqique, S.; Zhu, H. Nanomaterials, nanofillers, and nanocomposites: Types and properties. In *Health and Environmental Safety of Nanomaterials*; Elsevier: Amsterdam, The Netherlands, 2021; pp. 3–37.
48. Li, F.; Josephson, D.P.; Stein, A. Colloidal assembly: The road from particles to colloidal molecules and crystals. *Angew. Chem. Int. Ed.* **2011**, *50*, 360–388. [[CrossRef](#)] [[PubMed](#)]
49. Ebrahimi, K.; Shiravand, S.; Mahmoudvand, H. Biosynthesis of copper nanoparticles using aqueous extract of *Capparis spinosa* fruit and investigation of its antibacterial activity. *Marmara Pharm. J.* **2017**, *21*, 866–871. [[CrossRef](#)]
50. Barreira, S.; Moutinho, C.; Silva, A.M.; Neves, J.; Seo, E.-J.; Hegazy, M.-E.F.; Efferth, T.; Gomes, L.R. Phytochemical characterization and biological activities of green tea (*Camellia sinensis*) produced in the Azores, Portugal. *Phytomed. Plus* **2021**, *1*, 100001. [[CrossRef](#)]
51. Suárez-Cerda, J.; Espinoza-Gómez, H.; Alonso-Núñez, G.; Rivero, I.A.; Gochi-Ponce, Y.; Flores-López, L.Z. A green synthesis of copper nanoparticles using native cyclodextrins as stabilizing agents. *J. Saudi Chem. Soc.* **2017**, *21*, 341–348. [[CrossRef](#)]
52. Asghar, M.A.; Asghar, M.A. Green synthesized and characterized copper nanoparticles using various new plants extracts aggravate microbial cell membrane damage after interaction with lipopolysaccharide. *Int. J. Biol. Macromol.* **2020**, *160*, 1168–1176. [[CrossRef](#)]

Disclaimer/Publisher's Note: The statements, opinions and data contained in all publications are solely those of the individual author(s) and contributor(s) and not of MDPI and/or the editor(s). MDPI and/or the editor(s) disclaim responsibility for any injury to people or property resulting from any ideas, methods, instructions or products referred to in the content.